JPE 9-4-5

Quantitative Analysis and Comparisons between In-Phase Control and Energy-Optimized Control for Series Power Quality Controllers

Hunag Xinming*, Liu Jinjun†, and Zhang Hui*

†*School of Electrical Eng., Xi'an Jiaotong University, Xi'an, China

ABSTRACT

In-phase control and energy-optimized control are the two major control strategies proposed for series power quality controllers (SPQC). However quantitative analysis and comparison between these two control strategies is quite limited in previous publications. In this paper, an extensive quantitative analysis is carried out on these two control strategies through phasor diagram approach, and a detailed quantitative comparison is conducted accordingly. The load current is used as the reference phasor, and this leads to a simpler and clearer phasor diagram for the quantitative relationship. Subsequently detailed analysis of SPQC using in-phase control and energy-optimized control are provided respectively, under different modes both for under voltage/voltage sag and for over voltage/voltage swell. The closed form analytic expressions and the curves describing SPQC compensation characteristics are obtained. The detailed system power flow is figured out for each mode, and the detailed quantitative comparison between the two control strategies is then carried out. The comparison covers several aspects of SPQC, such as required compensating voltage magnitude, required capacity of energy storage component, and maximal ride-through time. In the end, computer simulation and prototype experimental results are shown to verify the validity of all the analysis and the result of the comparison.

Keywords: In-phase control, Energy-optimized control, Series power quality controller, Phasor diagram, Quantitative

1. Introduction

Under voltage/voltage sag and over voltage/voltage swell are the most familiar voltage disturbances[1-2] in a distribution network, and voltage sag is the major source of power quality-related problems[3-4]. These cause many bad effects[5-6] on sensitive equipment, such as influencing its product quality even to the point of malfunction, consequently resulting in financial losses[7-8]. Therefore, cost effective solutions, which make sensitive equipment work properly in these disturbances, are required urgently by the industrial field. One such solution is the series power quality controller (SPQC), whose system configuration is shown in Fig. 1. It is inserted into the system between source and sensitive load, which outputs the desired compensating voltage to cancel out the voltage disturbances and regulate load voltage well.

There are several control strategies for SPQC, such as pre-fault control, in-phase control, and energy-optimized

Manuscript received Dec. 3, 2008; revised April 20, 2009
†Corresponding Author: jjliu@mail.xjtu.edu.cn
Tel: +86-29-82667858, Fax: +86-29-82665223, XJTU
*School of Electrical Eng., Xi'an Jiaotong University, Xi'an, China

control. Pre-fault control[9-10] compensates load voltage to its pre-fault state, both for magnitude and phase, but it is unnecessary for the load not so sensitive to phase angle shift[11-12]. In-phase control[13-14] regulates load voltage to the desired magnitude and in-phase with the source voltage. It is widely used in industrial applications due to its easy analysis and implementation. Much active power is required in compensation, so high rating energy storage equipment is essential, and thus the increased cost. Energy-optimized control[15-18] aims at compensating disturbances with zero or minimal active power injection, which claims to have improved performance in DC energy usage and prolonged maximal ride-through time, thereby greatly reducing high cost for the high rating energy storage equipment. Among these control strategies, a simple comparison for in-phase control and energy-optimized control was first done in [19], though only for injection apparent power in voltage sag. A further comparison was done in [20], where compensating voltage magnitude and rating are deduced by complex mathematical method. This was done further in [21] with more comparison parameters. However, quantitative comparisons between them are hard to obtain since most existing results were obtained from the complex mathematical deduction. The process is not straightforward and the results are obscure, so less physical meaning existed. Most comparisons were partially done in under voltage/voltage sag only, even only in zero active power injection mode[18]. The quantitative analysis and comparison are carried out for SPQC between in-phase control and energy-optimized control more extensively in this paper.

The main ideal and corresponding phasor diagram are first discussed for each control strategy in section II, where load current is chosen as the reference for a simpler and clearer phasor diagram on the quantitative relationship. Subsequently detailed analysis of SPQC using respective in-phase and energy-optimized control are provided, under different modes for both under voltage/voltage sag and over voltage/voltage swell, and the detailed quantitative comparison between control strategies is then carried out accordingly in section III, where the closed form analytic expression and the curves describing SPQC compensation characteristics are obtained, and the system detailed power flow is figured out further. In section IV, SPQC maximal ride-through time is deduced and compared extensively by using both control strategies. The computer simulation and prototype experimental results are shown to verify the validity of all analysis and comparisons in section V. Finally the conclusions are summarized.

2. Phasor Diagram Analysis

The load current is chosen as reference phasor in this paper, and the common RL load is chosen in the analysis.

2.1 Both strategies control model

In both control strategies, SPQC is controlled as one controllable voltage source, which outputs the required voltage to cancel voltage disturbances and regulate load voltage well. The analysis defines source voltage as $\dot{U}_S$, regulated load voltage as $\dot{U}_L$, and compensating voltage as $\dot{U}_C$. The whole system model in the equivalent circuit format is obtained as shown in Fig. 2.

From this system model, once the load and source voltage phasor is determined, the SPQC compensating voltage phasor is obtained accordingly. Phase and magnitude of source voltage can be detected, and load voltage magnitude is a determined value. Once the load voltage phase is determined, SPQC compensating voltage can be obtained accordingly.

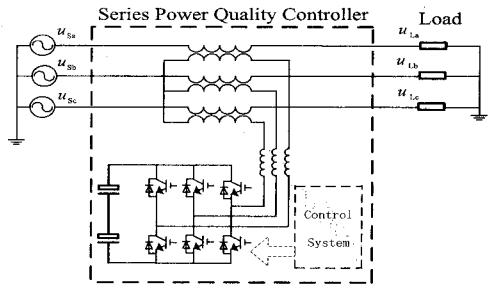

Fig. 1. The system configuration of SPQC.

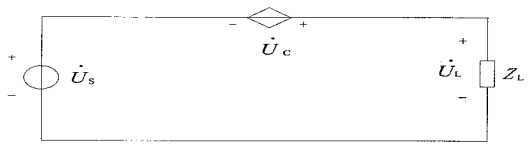

Fig. 2. Whole system model in the equivalent circuit format.

2.2 In-phase control

When in under voltage/voltage sag, the regulated load voltage is in-phase with source voltage, and compensating voltage is in-phase also. The phasor diagram for this case is as shown in Fig. 3, from which compensating voltage magnitude is proportional to source voltage disturbance degree, and thus injected active power. For this reason, the large and expensive energy storage equipment is essential for SPQC in this case, which leads to the increased costs.

When over voltage/voltage swell occurs, load voltage is in-phase with source voltage, but compensating voltage has the reverse-phase. The phasor diagram for this state is shown in Fig. 4, where compensating voltage magnitude is proportional to source voltage disturbance degree too, and thus the absorbed excessive active power. This absorbed excessive active power should be dealt with carefully[22-23], so system complexity and total cost is increased dramatically.

The control method for in-phase control is shown in Fig. 5. Where load voltage phase is calculated first, so the desired load voltage is formulated accordingly. The SPQC compensating voltage reference is obtained by subtracting the desired load voltage from detected source voltage. SPQC output voltage tracking control is used for better results.

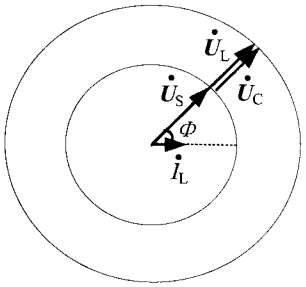

Fig. 3. Phasor diagram in under voltage/voltage sag.

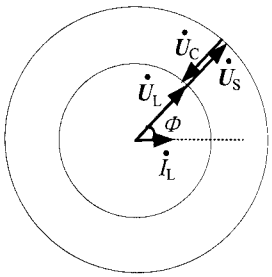

Fig. 4. Phasor diagram in over voltage/voltage swell.

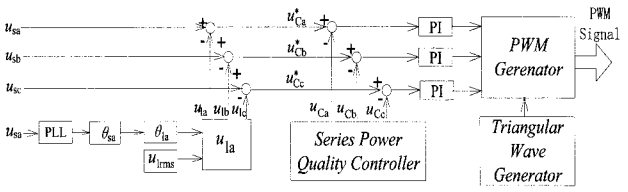

Fig. 5. Control method for SPQC with in-phase control.

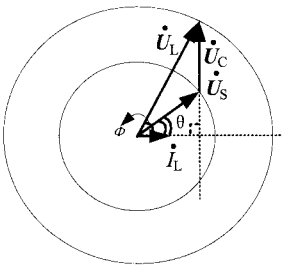

Fig. 6. Phasor diagram for zero active power injection mode.

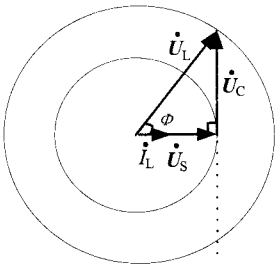

Fig. 7. Phasor diagram for boundary mode.

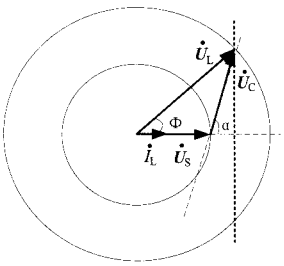

Fig. 8. Phasor diagram for the minimal active power injection mode.

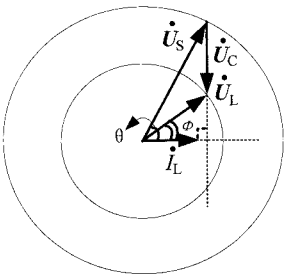

Fig. 9. Phasor diagram for over voltage/voltage swell.

2.3 Energy-optimized control

Energy-optimized control regulates load voltage with zero or minimal active power injection. SPQC works in zero active power injection mode, boundary mode, and minimal active power injection mode respectively[18] with different conditions in under voltage/voltage sag.

When SPQC works in zero active power injection mode, its compensating voltage is perpendicular to load current, so it only generates reactive power. The source provides all the active power in addition to the inadequate reactive power for the load. The phasor diagram for this mode is shown in Fig. 6, where the smaller compensating voltage is chosen to reduce SPQC system rating requirement.

When the under voltage/voltage sag deepens, SPQC works in boundary mode. Here the compensating voltage is perpendicular to the load current, and the source voltage is in-phase with the load current simultaneously. So SPQC only generates reactive power and the source provides active power only, which are combined to feed the load. The phasor diagram for this mode is shown in Fig. 7, where the phase difference between source voltage and load voltage equals the load power factor angle.

When SPQC works in minimal active power injection mode, source voltage is still in-phase with load current, but the compensating voltage is not perpendicular to load current any longer. Here the source generates active power only. SPQC generates the inadequate active power and all the reactive power to the load. The phasor diagram for this minimal active power injection mode is shown in Fig. 8, where the phase difference equals the load power factor angle also. As active power needed by the load is a fixed value and generated by the source maximally, SPQC only generates minimal active power in the compensation, and the name for this mode is formed.

For over voltage/voltage swell, SPQC only works in the other zero active power injection mode[18]. This mode is similar to the zero active power injection mode in under voltage/voltage sag, but compensating voltage has a reverse direction perpendicular to load current, and source power factor is smaller also. Here source generates all the active power in addition to excessive reactive power, and SPQC functions to absorb this excessive reactive power only. The phasor diagram for this mode is shown in Fig. 9, where the smaller compensating voltage is chosen for a smaller system power rating requirement also.

So energy storage equipment is reduced greatly in under voltage/voltage sag, as none or minimal active is needed. No additional actions are needed for excessive active power in over voltage/voltage swell, thus excessive cost is reduced remarkably for the energy-optimized control.

However, phase angle change between the source voltage and the load voltages is introduced by the control itself. This prohibits its application in the loads that are sensitive to phase angle shift. Almost all voltage disturbances are associated with some degree phase shift[11-12], and proper actions[24-25] can be taken to alleviate its bad effects, so this energy-optimized control strategy is considered to be one of the most promising strategies.

The control method for energy-optimized control is the same as Fig. 5, except for obtaining the desired load voltage phase. Source power factor angle is obtained for each mode first from the phasor diagram shown in Fig. 6-9. Load power factor angle can be changed and detected if needed, but it is predetermined and fixed in analysis and following control here. From these results, phase difference between source voltage and load voltage is obtained easily. The source voltage phase is detected in the control, and the desired load voltage phase is obtained by adding the phase difference to the obtained desired load voltage phase. This desired load voltage phase is combined with desired load voltage magnitude to get desired load voltage accordingly.

3. Quantitative Analysis and Comparisons

Per unit is used in quantitative analysis, and load current and desired load voltage are chosen as the base for current and voltage respectively in the analysis. RL load with the same parameters is chosen, so active and reactive power needed by the load is the same for both control strategies as follows.

$$\begin{cases} P_L^* = \cos\phi \\ Q_L^* = \sin\phi \end{cases} \tag{1}$$

3.1 Under voltage/voltage sag

According to Fig. 2, the compensating voltage of SPQC

with in-phase control is obtained.

$$U_C^* = 1 - U_S^* \tag{2}$$

Similarly, the active and reactive power generated by SPQC is shown as follows.

$$\begin{cases} P_C^* = (1 - U_S^*)\cos\phi \\ Q_C^* = (1 - U_S^*)\sin\phi \end{cases} \tag{3}$$

According to (2) and (3), SPQC graphical compensating voltage magnitude and injecting active power is shown in Fig. 10 (a) and (b) respectively. In each figure, the x axis is load power factor, y axis is source voltage magnitude, z axis is compensating voltage magnitude or injecting active power respectively. The axes definitions are similar for the following Fig. 12, Fig. 15, Fig. 17, Fig. 18, Fig. 20 and Fig. 22, though with minor differences.

With the same method, active and reactive power provided by the source is obtained also.

$$\begin{cases} P_S^* = U_S^* \cos\phi \\ Q_S^* = U_S^* \sin\phi \end{cases} \tag{4}$$

From (1), (3) and (4), the system power flow is figured out as shown in Fig. 11, where active and reactive power generated or absorbed by each part is proportional to its receiving voltage.

For the energy-optimized control, when SPQC works in zero active power injection mode, the following relationship is obtained easily from Fig. 6.

$$U_S^* > \cos\phi \tag{5}$$

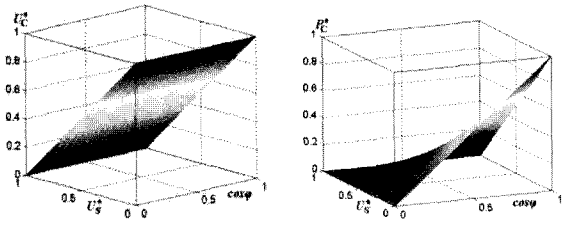

(a) Injecting active power (b) Compensating voltage magnitude

Fig. 10. Quantitative analysis for in-phase control.

And SPQC compensating voltage magnitude is obtained as follows accordingly.

$$U_C^* = \sin\phi - \sqrt{(U_S^*)^2 - \cos^2\phi} \tag{6}$$

SPQC graphical compensating voltage magnitude is obtained as shown in Fig. 12.

SPQC generated active and reactive power is obtained easily as follows. Comparing the obtained reactive power with (6), it can be found that SPQC generated reactive power equals its compensating voltage magnitude in obtained per unit expression.

$$\begin{cases} P_C^* = 0 \\ Q_C^* = \sin\phi - \sqrt{(U_S^*)^2 - \cos^2\phi} \end{cases} \tag{7}$$

Similarly, the active and reactive power provided by the source is shown as follows.

$$\begin{cases} P_S^* = \cos\phi \\ Q_S^* = \sqrt{(U_S^*)^2 - \cos^2\phi} \end{cases} \tag{8}$$

From (1), (7) and (8), system power flow for this mode is figured out as shown in Fig. 13.

When SPQC works in boundary mode, the following relationship is obtained from Fig. 7.

$$U_S^* = \cos\phi \tag{9}$$

So SPQC compensating voltage magnitude is shown as follows, which is a space curve only.

$$U_C^* = \sin\phi \tag{10}$$

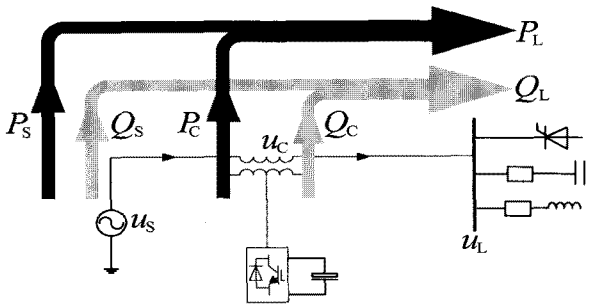

Fig. 11. System power flow for in-phase control.

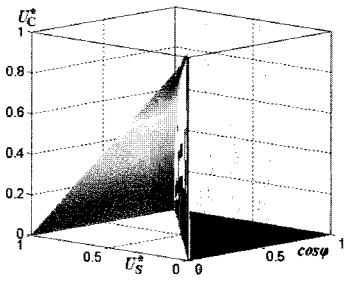

Fig. 12. Compensating voltage magnitude for the zero active power injection mode.

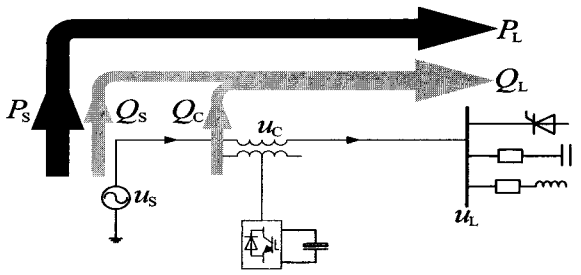

Fig. 13. System power flow for the zero active power injection mode.

SPQC generated active and reactive power is obtained easily as follows. It proves SPQC generates reactive power only, which equals load needed instantaneously.

$$\begin{cases} P_C^* = 0 \\ Q_C^* = \sin\phi \end{cases} \tag{11}$$

Similarly, the active and reactive power provided by the source is shown as follows. It proves source generates active power only, and it is equal to load needed also.

$$\begin{cases} P_S^* = \cos\phi \\ Q_S^* = 0 \end{cases} \tag{12}$$

From (1), (11) and (12), the system power flow for this mode is figured out as shown in Fig. 14.

When SPQC works in minimal active power injection mode, the following relationship is obtained easily from its phasor diagram shown in Fig. 8.

$$U_S^* < \cos\phi \tag{13}$$

SPQC compensating voltage magnitude is obtained accordingly.

$$U_C^* = \sqrt{1+\left(U_S^*\right)^2 - 2U_S^*\cos\phi} \tag{14}$$

Similarly, SPQC generated active and reactive power is obtained as follows. The obtained reactive power equals compensating voltage magnitude per unit also.

$$\begin{cases} P_C^* = \cos\phi - U_S^* \\ Q_C^* = \sin\phi \end{cases} \tag{15}$$

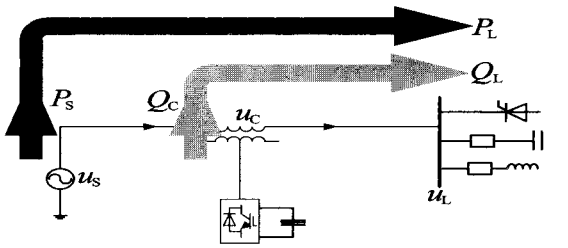

Fig. 14. System power flow for the boundary mode.

Based on (14) and (15), SPQC graphical compensating voltage magnitude or injecting active power is shown in Fig. 15 (a) and (b) respectively.

The active and reactive power generated by the source is similarly obtained as follows.

$$\begin{cases} P_S^* = U_S^* \\ Q_S^* = 0 \end{cases} \tag{16}$$

From (1), (15) and (16), the system power flow for this mode is figured out as follows.

By comparing SPQC compensating voltage magnitude between control strategies shown in (2), (6), (10) and (14) respectively, it is larger for energy-optimized control. The corresponding graphical larger part for energy-optimized control is shown in Fig. 17 (a). This larger magnitude makes SPQC required power rating larger.

While comparing SPQC injecting active power using both control strategies shown in (3), (7), (11) and (15) respectively, it is smaller for the energy-optimized control. The corresponding graphical smaller part for SPQC using energy-optimized control is shown in Fig. 17 (b), so SPQC requires a smaller capacity energy storage component also.

In summary, SPQC with energy-optimized control has

larger compensating voltage magnitude, and thus a larger required power rating. But it requires much less active power, and requires smaller energy storage component capacity accordingly, thus resulting in reduced cost.

3.2 Over voltage/voltage swell

According to Fig. 4, compensating voltage magnitude of SPQC with in-phase control is obtained as follows.

$$U_C^* = U_S^* - 1 \tag{17}$$

Similarly, SPQC absorbed active and reactive power is shown as follows.

$$\begin{cases} P_C^* = (1 - U_S^*)\cos\phi \\ Q_C^* = (1 - U_S^*)\sin\phi \end{cases} \tag{18}$$

SPQC graphical compensating voltage magnitude or absorbed active power is shown in Fig. 18 (a) and (b) respectively as follows.

Using the same method, the active and reactive power generated by the source is obtained also as follows.

$$\begin{cases} P_S^* = U_S^* \cos\phi \\ Q_S^* = U_S^* \sin\phi \end{cases} \tag{19}$$

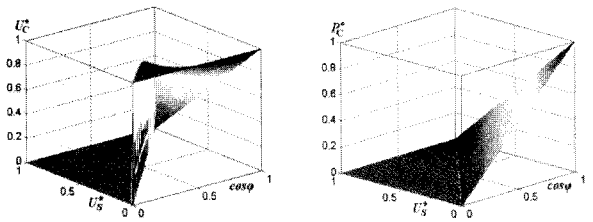

(a) Compensating voltage magnitude (b) Injecting active power

Fig. 15. Quantitative analysis for the minimal active power injection mode.

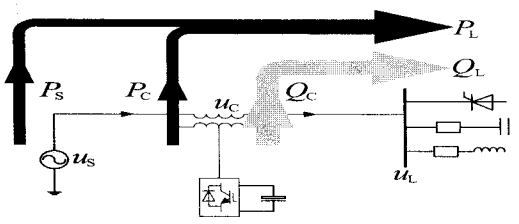

Fig. 16. System power flow in minimal active power injection. mode.

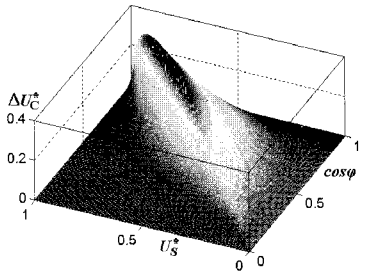

(a) Compensating voltage magnitude quantitative difference

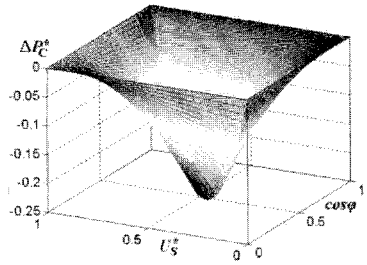

(b) Quantitative difference in the injecting active power

Fig. 17. Quantitative difference between the energy-optimized control and the in-phase control in under voltage/voltage sag.

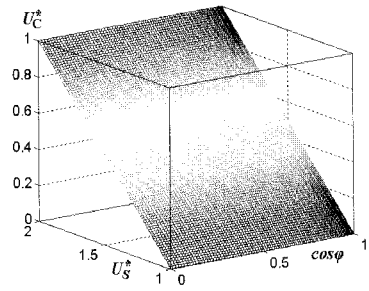

(a) Compensating voltage magnitude

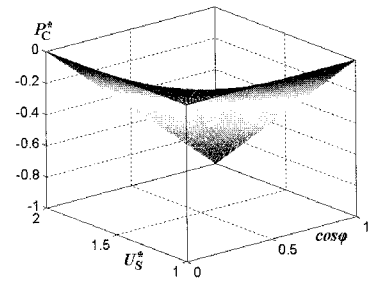

(b) Absorbed active power

Fig. 18. Quantitative analysis for in-phase control.

From (1), (18) and (19), the system power flow is figured out accordingly as shown in Fig. 19.

According to Fig. 9, compensating voltage magnitude of SPQC with energy-optimized control is obtained easily, which is shown as follows.

$$U_C^* = \sqrt{\left(U_S^*\right)^2 - \cos^2\phi} - \sin\phi \tag{20}$$

SPQC graphical compensating voltage magnitude is obtained accordingly as shown in Fig. 20.

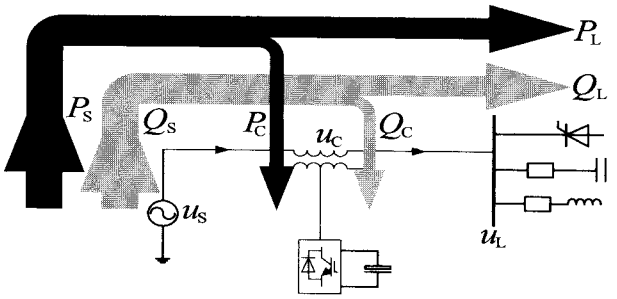

Fig. 19. System power flow for in-phase control.

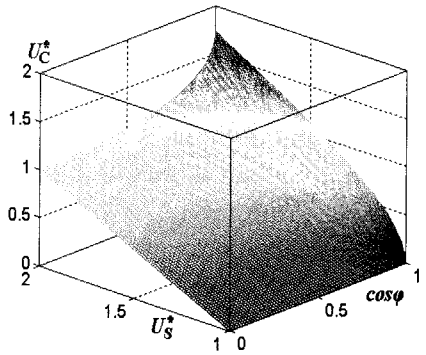

Fig. 20. Compensating voltage magnitude in energy-optimized control at over voltage/voltage swell.

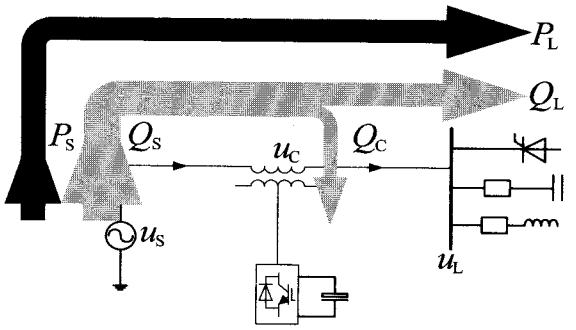

Fig. 21. System power flow for energy-optimized control.

Similarly, the active and reactive power absorbed by SPQC is obtained as follows.

$$\begin{cases} P_C^* = 0 \\ Q_C^* = \sqrt{\left(U_S^*\right)^2 - \cos^2\phi} - \sin\phi \end{cases} \tag{21}$$

The active and reactive power generated by the source is shown as follows.

$$\begin{cases} P_S^* = \cos\phi \\ Q_C^* = \sqrt{\left(U_S^*\right)^2 - \cos^2\phi} \end{cases} \tag{22}$$

From (1), (21) and (22), the system power flow for this mode is figured out as follows.

By comparing SPQC compensating voltage magnitude shown in (17) and (20), it is larger in energy-optimized control, and the corresponding graphical larger part is shown in Fig. 22. So the required power rating is larger also.

While comparing SPQC absorbed active power in both control strategies shown in (18) and (21), SPQC with energy-optimized control does not absorb any excessive active power, so no additional actions[22-23] are needed for system safe operation, and the cost for this is avoided also.

In summary, SPQC with energy-optimized control has larger compensating voltage magnitude, and thus required power rating. But it requires zero or minimal active power in under voltage/voltage sag compensation, and thus requires much less capacity of energy storage component; this does not absorb excessive active power in over voltage/voltage swell, so no additional action is needed for system safe operation. Therefore the cost for both is reduced dramatically.

4. SPQC Maximal Ride-through Time

SPQC maximal ride-through time is determined by the required active power and the capacity of energy storage component. Only the DC capacitor is served as energy storage equipment in the analysis here. The DC voltage maximal fluctuation range is defined to be 85%~110% of the desired value, and the corresponding maximal ride-through time can be defined as follows, which includes the DC voltage decrease and increase conditions respectively.

$$t_{\max}=\frac{W_{C\max}}{P}=\begin{cases}\dfrac{\frac{1}{2}CU_{DC0}^2-\frac{1}{2}CU_{DC\min}^2}{P_C+P_{Loss}} & U_{DC}<U_{DC0}\\ \dfrac{\frac{1}{2}CU_{DC\max}^2-\frac{1}{2}CU_{DC0}^2}{P_C-P_{Loss}} & U_{DC}<U_{DC0}\end{cases} \tag{23}$$

4.1 Under voltage/voltage sag

From the above definition, the maximal ride-through time for SPQC with in-phase control is obtained as follows.

$$t_{\max}=\frac{W_{C\max}}{P}=\frac{\frac{1}{2}CU_{DC0}^2-\frac{1}{2}C\left(0.85\times U_{DC0}\right)^2}{\left(U_L-U_S\right)I_L\cos\phi+P_{Loss}}=\frac{0.2775\times\frac{1}{2}CU_{DC0}^2}{\left(U_L-U_S\right)I_L\cos\phi+P_{Loss}} \tag{24}$$

As for energy-optimized control, maximal ride-through time for SPQC works in zero active power injection mode and boundary mode is obtained as follows, where no active power is needed in the compensation itself.

$$t_{\max}=\frac{W_{C\max}}{P}=\frac{\frac{1}{2}CU_{DC0}^2-\frac{1}{2}C\left(0.85\times U_{DC0}\right)^2}{P_{Loss}}=\frac{0.2775\times\frac{1}{2}CU_{DC0}^2}{P_{Loss}} \tag{25}$$

Similarly, maximal ride-through time for SPQC work in minimal active power injection mode is as follows.

$$t_{\max}=\frac{W_{C\max}}{P}=\frac{\frac{1}{2}CU_{DC0}^2-\frac{1}{2}C\left(0.85\times U_{DC0}\right)^2}{U_LI_L\cos\phi-U_SI_L+P_{Loss}}=\frac{0.2775\times\frac{1}{2}CU_{DC0}^2}{U_LI_L\cos\phi-U_SI_L+P_{Loss}} \tag{26}$$

By comparing (25) and (26) with (24), SPQC with energy-optimized control has larger maximal ride-through time in under voltage/voltage sag compensation.

4.2 over voltage/voltage swell

Maximal ride-through time for SPQC with in-phase control is obtained as follows, where it absorbs excessive active power, so the DC voltage is increased.

$$t_{\max}=\frac{W_{C\max}}{P}=\frac{\frac{1}{2}C\left(1.1\times U_{DC0}\right)-\frac{1}{2}CU_{DC0}^2}{P_C-P_{Loss}}=\frac{0.21\times\frac{1}{2}CU_{DC0}^2}{\left(U_S-U_L\right)I_L\cos\phi-P_{Loss}} \tag{27}$$

Similarly, maximal ride-through time for SPQC with energy-optimized control is obtained as follows.

$$t_{\max}=\frac{W_{C\max}}{P}=\frac{\frac{1}{2}CU_{DC0}^2-\frac{1}{2}C\left(0.85\times U_{DC0}\right)}{P_{Loss}}=\frac{0.2775\times\frac{1}{2}CU_{DC0}^2}{P_{Loss}} \tag{28}$$

By comparing (28) with (27), the numerator in (28) is larger clearly. System power loss is usually much smaller compared with required active power itself, so it can be considered that the denominator in (28) is less than (27) also. So the maximal ride-through time for SPQC with energy-optimized control is also larger in over voltage/voltage swell compensation.

In summary, maximal ride through time for SPQC using energy-optimized control is larger than using in-phase control in both under voltage/voltage sag compensation, and over voltage/voltage swell compensation.

5. Simulation and Experimental Verifications

For simple implementation and comparison, three phase balanced RL load with 9.42Ω resistor and 30mH inductor is chosen for both control strategies in both computer simulation and prototype experiment. The load power factor angle is 45°, which is considered the known parameter for energy-optimized control.

Similarly, voltage sag and swell is generated on purpose. The voltage sag degree is 20%, 30% and 40% respectively, and the voltage swell degree is 20% in both the computer simulation and the prototype experiment for both control strategies. In each obtained figure, four signals are detected, with source voltage, compensating voltage, load voltage and load current in descending order.

5.1 Computer simulation

The desired load voltage is 220V RMS. Voltage disturbance happens at 0.14S, lasting 6 cycles and ends at 0.26S in the computer simulation done in PSIM 4.1.

The corresponding obtained computer simulation results for SPQC with in-phase control and energy-optimized control in each voltage disturbance are shown in Fig. 23 and 24 respectively.

From Fig. 23, it can be found that when SPQC uses in-phase control, disturbances are compensated and load voltage is regulated well. Additionally, source voltage is in-phase with load voltage, SPQC compensating voltage is in-phase with load voltage also in under voltage/voltage

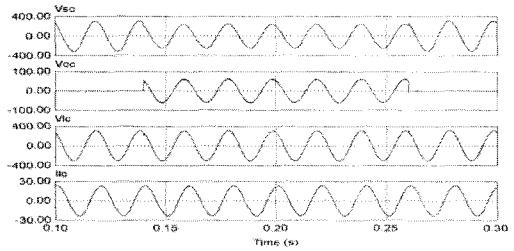

(a) 20% voltage sag

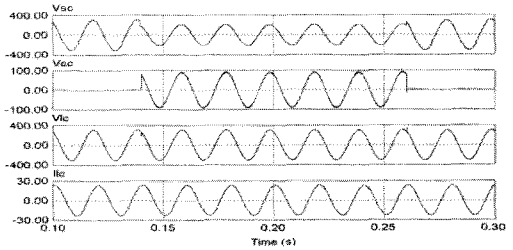

(b) 30% voltage sag

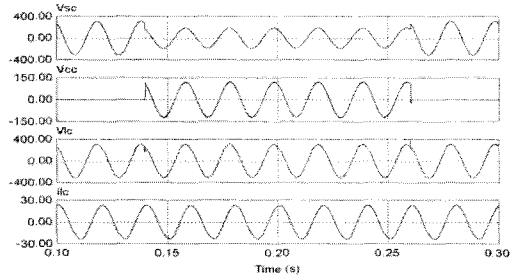

(c) 40% voltage sag

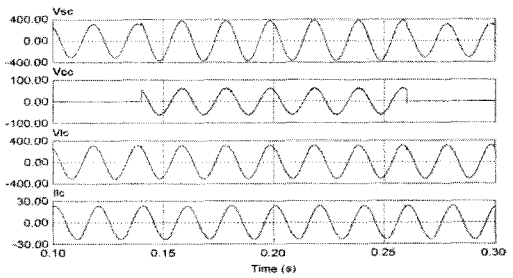

(d) 20% voltage swell

Fig. 23. Simulation results for in-phase control.

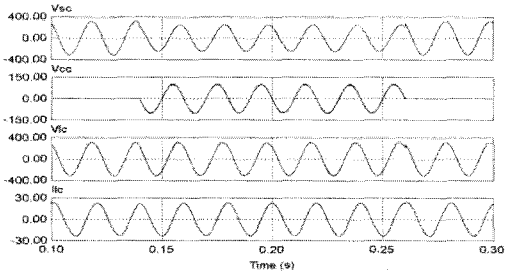

(a) 20% voltage sag

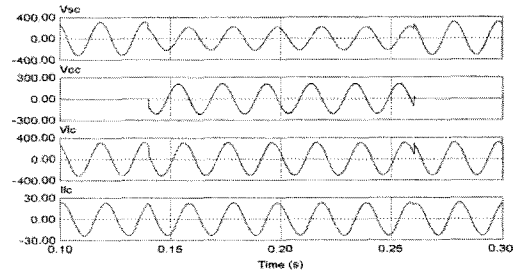

(b) 30% voltage sag

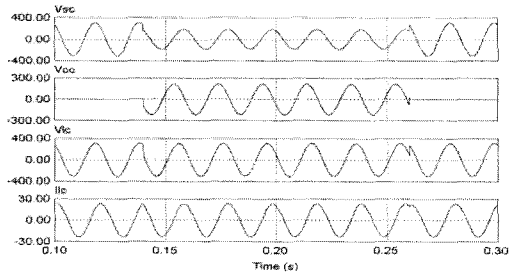

(c) 40% voltage sag

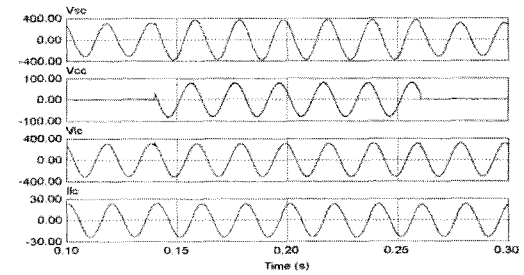

(d) 20% voltage swell

Fig. 24. Simulation results for energy-optimized control.

sags while in reverse-phase in over voltage/voltage swell. All the results match in-phase control characteristics well.

From Fig. 24, it can be found that when SPQC uses energy-optimized control, it works in four different modes respectively in the compensation. Voltage disturbances are compensated and thus load voltage is regulated well. In addition, SPQC compensating voltage is leading 90° to load current in Fig. 24(a). SPQC compensating voltage is leading 90° to the load current, and source voltage is in-phase with load current simultaneously in Fig. 24(b). While only source voltage is in-phase with the load current in Fig. 24(c), without 90° phase is a different relationship between load and source voltage. Conversely, SPQC compensating voltage is lagging 90° to load current

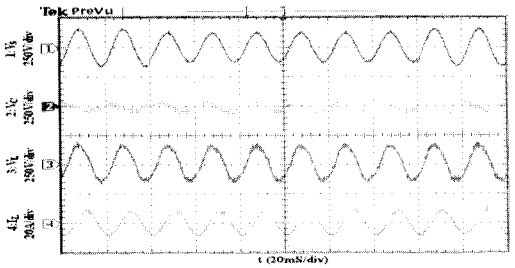

(a) 20% voltage sag

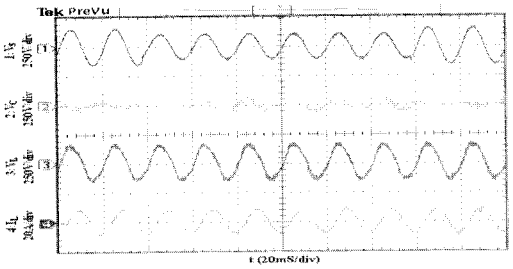

(b) 30% voltage sag

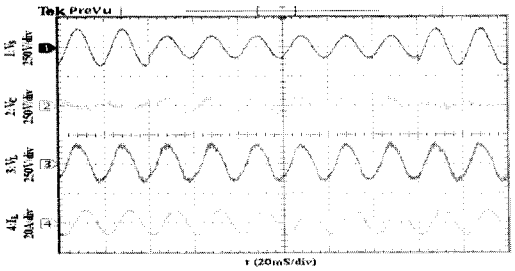

(c) 40% voltage sag

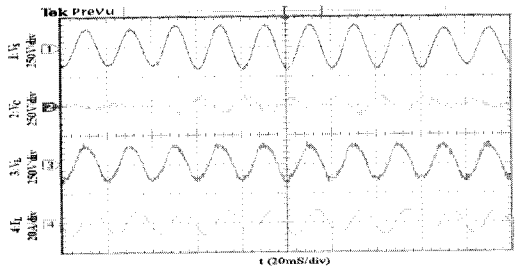

(d) 20% voltage swell

Fig. 25. Experimental results for in-phase control.

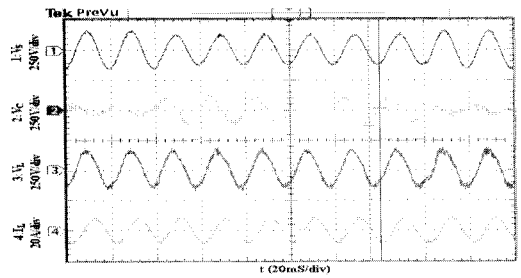

(a) 20% voltage sag

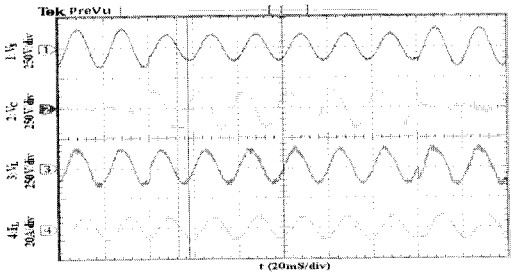

(b) 30% voltage sag

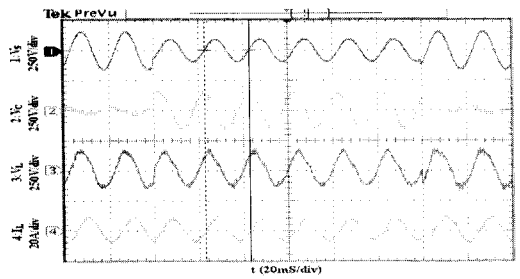

(c) 40% voltage sag

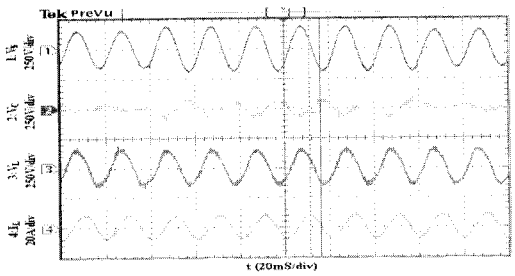

(d) 20% voltage swell

Fig. 26. Experimental results for energy-optimized control.

in Fig. 24 (d). All these results match the characteristics of corresponding modes in energy-optimized control well.

By comparing the same voltage disturbance compensated by SPQC with in-phase control and energy-optimized control respectively in Fig. 23 and 24 further, SPQC with energy-optimized control has larger compensating voltage magnitude in all four cases, so the required rating for SPQC using energy-optimized control is larger also.

5.2 Prototype experiment

In prototype experiment, the desired load voltage is 110V RMS. 6 cycles balanced disturbances are generated by programmable AC power supply with every 100 normal voltage cycles in each sequence. All the other parameters are the same as the computer simulation.

Prototype experimental results for SPQC with in-phase and energy-optimized control in each voltage disturbance are obtained and shown in Fig. 25 and 26 respectively.

By carefully comparing respective experimental results, and comparing the corresponding simulation results, similar conclusions can be obtained as in the simulation results analysis. All experimental results coincide with the corresponding simulation results well. Both of them verify the validity of the characteristics and comparison results of corresponding control strategy well.

6. Conclusions

In this paper, an extensive analysis and comparison are done between in-phase control and energy-optimized control of SPQC based on the phasor diagram method. Load current is used as a reference phasor in the analysis. Closed form analytic expressions and curves describing SPQC compensation characteristics are obtained for both control strategies. Computer simulation and prototype experiment are done to verify the validity of all analysis and control. The following results are obtained by comparing them.

1) Quantitative closed form analytic expressions using system parameters and curves describing SPQC needing active power are obtained and compared in both control strategies. SPQC using energy-optimized control requires zero or minimal active power in the compensation, so less energy storage equipment is used in under voltage/voltage sag and no extra actions are needed for over voltage/voltage swell resulting in reduced cost.

2) Quantitative closed form analytic expressions with system parameters and curves describing SPQC required compensating voltage magnitude in both control strategies are obtained and compared. SPQC using energy-optimized control requires larger amplitude of compensating voltage, so its required power rating is larger also.

3) Quantitative closed form analytic expressions using system parameters describing SPQC maximal ride-through time in both control strategies are obtained and compared. SPQC with Energy-optimized control has longer maximal ride-though time than in-phase control.

Acknowledgment

This work is sponsored by the National Key Technology R&D Program in the 11th Five year Plan of China (2007BAA12B03).

References

[1] D.O. Koval, R.A. Bocancea, Yao Kai, M.B. Hughes, "Canadian national power quality survey: frequency and duration of voltage sags and surges at industrial sites," *IEEE Trans. Ind. Appl.*, Vol. 34, No. 5, pp. 904-910, 1998.

[2] D.S. Dorr, M.B. Hughes, T.M. Gruzs, R.E. Jurewicz, J.L. McClaine, "Interpreting recent power quality surveys to define the electrical environment," *IEEE Trans. Ind. Appl.*, Vol. 33, No. 6, pp. 1480-1487, 1997.

[3] E.W. Gunther, H. Mebta, "A survey of distribution system power quality-preliminary results," *IEEE Trans. on Power Delivery*, Vol. 10, No. 1, pp. 322-329, 1995.

[4] D.O. Koval, J. Leonard, Z.J. Licsko, "Power quality of small rural industries," *IEEE Trans. Ind. Appl.*, Vol. 29, No. 4, pp. 696-700, 1993.

[5] M.H.J. Bollen, "Voltage sags: effects, mitigation and prediction," *Power Engineering Journal*, Vol. 10, No. 3. pp. 129-135, 1996.

[6] A. Polycarpou, H. Nouri, T. Davies, R. Ciric, "An overview of voltage sag theory, effects and equipment compatibility," *in Proc. of UPEC 2004*, Vol. 3, pp. 966-972, 2004.

[7] R.C. Degeneff, R. Barss, D. Carnovale, S. Raedy, "Reducing the effect of sags and momentary interruptions: a total owning cost prospective," *in Proc. of ICHQP*, Vol. 2, pp. 397-403, 2000.

[8] C.P. Gupta, J.V. Milanovic, M.T. Aung, "The influence of process equipment composition on financial losses due to voltage sags", *in Proc. of ICHQP*, pp. 28-34, 2004.

[9] E.K.K. Sng, S.S. Choi, D.M. Vilathgamuwa, "Analysis of series compensation and DC-link voltage controls of a transformerless self-charging dynamic voltage restorer," *IEEE Trans. on Power Delivery*, Vol. 19, No. 3, pp. 1511-1518, 2004.

[10] A.K. Ramasamy, R. Krishnan Iyer, V.K. Ramachandaramuthy, R.N. Mukerjee, "Dynamic Voltage Restorer for Voltage Sag Compensation," *in Proc. of PEDS*, Vol. 2, pp. 1289-1294, 2005.

[11] S.W. Middlekauff, E.R. Collins Jr., "System and customer impact: considerations for series custom power devices," *IEEE Trans. Power Delivery*, Vol. 13, No. 1, pp. 278-282, 1998.

[12] J.D. Li, S.S. Choi, D.M. Vilathgamuwa, "Impacts of Voltage phase shift on motor loads and series custom power devices including converter thermal effects," *IEEE Trans. on Power Delivery*, Vol. 19, No. 4, pp. 1941-1949, 2004.

[13] C.J. Zhan, V.K. Ramachandaramurthy, A. Arulampalam, C. Fitzer, S. Kromlidis, M. Bames, N. Jenkins, "Dynamic voltage restorer based on voltage-space-vector PWM control," *IEEE Trans. Ind. Appl.*, Vol. 37, No. 6, pp. 1855-1863, 2001.

[14] J.G. Nielsen, M. Newman, H. Nielsen, F. Blaabjerg, "Control and testing of a dynamic voltage restorer (DVR) at medium voltage level," *IEEE Trans. Power Electronics*, Vol. 19, No. 3, pp. 806-813, 2004.

[15] M. Vilathgamuwa, A.A.D. Ranjith Perera, S.S. Choi and K.J. Tseng, "Control of energy optimized dynamic voltage restorer," *in Proc. of IECON*, Vol. 2, pp. 873-878, 1999.

[16] M.H. Haque, "Voltage sag correction by dynamic voltage restorer with minimum power injection," *IEEE Power Eng. Review*, Vol. 21, No. 5, pp. 56~58, 2001.

[17] D.M. Vilathgamuwa, A.A.D.R. Perera and S.S. Choi, "Voltage sag compensation with energy optimized dynamic voltage restorer," *IEEE Trans. on Power Delivery*, Vol. 18, No. 3, pp. 928~936, 2003.

[18] X.M. Huang, J.J. Liu, H. Zhang, "Quantitative Analysis on Different Modes of Energy Optimal Control for Series Power Quality Controllers," *in Proc. of CES/IEEE IPEMC*, Vol. 3, pp. 1497-1501, 2006.

[19] M.H. Haque, "Compensation of distribution system voltage sag by DVR and D-STATCOM", *in proc. of IEEE Porto Power Tech*, Vol. 1, pp. 1-5, 2001.

[20] W. El-Khattam, M. Elnady, M.M.A. Salama, "Distributed generation impact on the dynamic voltage restorer rating," *in Proc. of IEEE/PES T&D expo*, Vol. 2, pp. 595-599, 2003.

[21] A. Moreno-Munoz, D. Oterino, M. Gonzalez, F.A. Olivencia, J.J. Gonzalez-de-la-Rosa, "Analysis of sag compensation with dynamic voltage restorer," *in Proc. of ISIE*, Vol. 3, pp. 1637-1641, 2006.

[22] H. Awad, F. Blaabjerg, "Mitigation of voltage swells by static series compensator," *in Proc. of PESC*, Vol. 5, pp. 3505-3511, 2004.

[23] G.C. Xiao, Z.L. Hu, C.H. Nan, Z.A. Wang, "DC-Link Voltage Pumping-up Analysis and Phase Shift Control for a Series Active Voltage Regulator," *in Proc. of PESC*, pp. 1-5, 2006.

[24] J.D. Li, S.S. Choi, D. Vilathgamuwa, "Impact of load transients on dynamic voltage restorers," *in Proc. of PowerCon*, Vol. 1, pp. 464-470, 2002.

[25] J.D. Li, S.S. Choi, D.M. Vilathgamuwa, "Impact of voltage phase jump on loads and its mitigation," *in Proc. of IPEMC*, Vol. 3, pp. 1762–1766, 2004.

Huang Xinming was born in Hubei, China in 1981. He received the B.S. degree from Xi'an Shiyou University, Xi'an, China, in 2003, and M.S. degree from Xi'an Jiaotong University, Xi'an, China, in 2006, both in Electrical Engineering, where he is currently pursuing the Ph.D. degree. His research interests include power-quality control, applications of power electronics in power systems, modeling and control of power-electronics circuits.

Liu Jinjun was born in Hunan, China in 1970. He received his B.S. and Ph.D. degrees in Electrical Engineering from Xi'an Jiaotong University (XJTU), China, in 1992 and 1997 respectively. After graduation he became a Lecturer at XJTU. From December 1999 until February 2002, he was with the Center for Power Electronics Systems at Virginia Polytechnic Institute and State University, USA, as a Postdoctoral Research Scholar. He then came back to XJTU and in August of 2002 was promoted to Full Professor and the head of the Power Electronics and Renewable Energy Center at XJTU. He has been serving as an Associate Dean of the Electrical Engineering School at XJTU since 2005. He has co-authored 3 books, published nearly 100 technical papers, and received several provincial or ministerial awards for scientific or career achievements and the 2006 Delta Scholar

Award. His research interests are power quality control, renewable energy generation and utility applications of power electronics, and modeling and control of power electronic systems. Dr. Liu is a member of China Electrotechnical Society (CES) and a member of China Power Supply Society (CPSS). He has been serving as the Deputy Secretary General of CES Power Electronics Society and the Deputy Secretary General of CPSS. Dr. Liu has also served as an AdCom member of the IEEE Power Electronics Society and an Associate Editor for the IEEE Transactions on Power Electronics.

Zhang Hui was born in Shaanxi, China, in 1982. He received the B.S. and M.S. degrees in Electrical Engineering from Xi'an Jiaotong University, Xi'an, China, in 2004 and 2007, respectively. Currently, he is an electrical engineer with Meiden Power Solutions, Singapore.